

E2-2013-103

O. O. Voskresenskaya, E. A. Kuraev, H. T. Torosyan

COULOMB CORRECTIONS
TO THE PARAMETERS OF THE
LANDAU-POMERANCHUK-MIGDAL EFFECT THEORY

Submitted to «Particles and Nuclei, Letters»

Воскресенская О. О., Кураев Э. А., Торосян Г. Т.
Кулоновские поправки к параметрам теории эффекта
Ландау–Померанчука–Мигдала

E2-2013-103

С использованием кулоновской поправки к углу экранирования теории многократного рассеяния Мольера аналитически и численно найдены кулоновские поправки для ряда параметров мигдаловской теории ЛПМ-эффекта. Показано, что полученная кулоновская поправка для спектральной плотности излучения электронов позволяет полностью преодолеть расхождение между предсказаниями теории ЛПМ эффекта и результатами его измерения.

Работа выполнена в Лаборатории теоретической физики им. Н. Н. Боголюбова ОИЯИ.

Препринт Объединенного института ядерных исследований. Дубна, 2013

Voskresenskaya O. O., Kuraev E. A., Torosyan H. T.
Coulomb Correction to the Parameters of the
Landau–Pomeranchuk–Migdal Effect Theory

E2-2013-103

Using the Coulomb correction to the screening angular parameter of the Molière multiple scattering theory, we obtained analytically and numerically the Coulomb corrections to the quantities of the Migdal LPM-effect theory. We showed that the Coulomb correction to the spectral bremsstrahlung rate allows completely eliminating the discrepancy between the predictions of the LPM effect theory and its measurements.

The investigation has been performed at the Bogoliubov Laboratory of Theoretical Physics, JINR.

Preprint of the Joint Institute for Nuclear Research. Dubna, 2013

INTRODUCTION

Landau and Pomeranchuk were the first to show [1] that multiplicity of electron scattering processes by atomic nuclei in an amorphous medium results in the suppression of soft bremsstrahlung. The quantitative theory of this phenomenon was created by Migdal [2, 3]*. Therefore, it received the name Landau–Pomeranchuk–Migdal (LPM) effect.

The next step in the development of the quantitative theory of the LPM effect was made in [5, 6] on the basis of the quasi-classical operator method in QCD. One of the basic equations of this method is the Schrödinger equation in the external field with an imaginary potential, which admits of formal solution in the form of the path integral [7]**. The same equation (without external field) was rederived in [8]. The last derivation is based on the approach which coincides basically with that of [6].

In [9] it was shown that analogous effects are possible also at coherent radiation of relativistic electrons and positrons in a crystalline medium, and the theory of these effects must also be based on the quasi-classical methods [9]. Effects of this kind should manifest themselves in scattering of protons by the nuclei, which has recently been shown in Groning by the AGOR collaboration [10], and penetration of quarks through the nuclear matter at the RHIC and LHC energies [11]. The QCD analog of the LPM effect was examined in [12]; a possibility studying the LPM effect in oriented crystal at GeV energy was analyzed in [13]; theoretically, an analogue of the LPM effect was considered for nucleon–nucleon collisions in the neutron stars and supernovae, and quark–gluon plasma [11, 14].

The results of a series of experiments at the SLAC [15, 16] and CERN-SPS [17, 18] accelerators on detection of the Landau–Pomeranchuk effect confirmed the basic qualitative conclusion that multiple scattering of ultrarelativistic charged particles in matter leads to suppression of their bremsstrahlung in the soft part of the spectrum. However, attempts to quantitatively describe the experimental data [15] faced an unexpected difficulty. For achieving satisfactory agree-

*See also [4] accounting the edge effects.

**In [7] an approach to the description of the LPM effect is developed where multiple scattering is described with the path integral treatment.

ment of data with theory [2], the authors [15] had to multiply the results in the Born approximation of their calculations by the normalization factor R equal to $0.94 \pm 0.01 \pm 0.032$, which had no reasonable explanation.

The alternate calculations [7, 8] gave a similar result despite different computational basis [15]. The theoretical predictions in agreement with the spectrum of 30 to 500 MeV photon bremsstrahlung measured for 25 GeV electron beam and 0.7–6.0% L_R gold target over the range $30 < \omega < 500$ MeV of the emitted photon frequency ω only within a normalization factor 0.93 [8] – 0.94 [15]. The origin of the above small but significant disagreement between data and theory needs to be better understood.

Considering the fact that the calculations for the description of the interaction of electrons with gold target atoms ($Z\alpha \sim 0.6$) in [8, 15, 16] were performed using the Born approximation, the above-mentioned discrepancy between theory and experiment can be explained at least qualitatively. The aim of this work is to show that the discussed discrepancy can also be explained quantitatively if the corrections to the results of the Born approximation (the so-called Coulomb corrections) are appropriately considered on the basis of a revised version of the Molière multiple scattering theory [19, 20].

The paper is organized as follows. In Sec. 1 we consider the basic formulae of the quantitative LPM effect theory for finite-size targets obtained by the kinetic equation method and also the small-angle approximation of this theory which is used further for analytical and numerical calculations. In Sec. 2 we present the results of the conventional [21] and a revised small-angle Molière multiple scattering theory applied in the next section to the theory of the LPM effect and its analogue for a thin target [22, 23]. In Sec. 3 we obtain the analytical and numerical results for Coulomb corrections to some quantities of the LPM effect theory for sufficiently thick targets and also to the asymptotes of the spectral radiation rate within its analogue for a thin layer of an amorphous medium. Finally, in Sec. 4 we briefly summarize our findings and state our conclusions.

1. LPM EFFECT THEORY FOR FINITE TARGETS

There exist two methods that allow one to develop a rigorous quantitative theory of the Landau–Pomeranchuk effect. This is Migdal’s method of kinetic equation [2, 3] and the method of functional integration [7, 8, 24]. Neglecting numerically small quantum-mechanical corrections, we will adhere to version of the Landau–Pomeranchuk effect theory, developed in [2, 4, 25].

1.1. Basic Formulae. Simple though quite cumbersome calculations using the results [2, 4] yield the following formula for the electron spectral bremsstrahlung intensity averaged over various trajectories of electron motion in the medium

(hereafter the units $\hbar = c = 1$, $e^2 = 1/137$ are used) [25]:

$$\begin{aligned} \left\langle \frac{dI}{d\omega} \right\rangle = & 2 \sum_{\epsilon} \left\{ n_0 L \int f^*(\mathbf{n}_2) \nu(\mathbf{n}_2 - \mathbf{n}_1) f(\mathbf{n}_1) d\mathbf{n}_1 d\mathbf{n}_2 - \right. \\ & - (n_0 v)^2 \int_0^T dt_1 \int_{t_1}^T dt_2 \operatorname{Re} \left[\int f^*(\mathbf{n}_2) \nu(\mathbf{n}_2 - \mathbf{n}'_2) f(\mathbf{n}_1) \times \right. \\ & \left. \left. \times \nu(\mathbf{n}'_1 - \mathbf{n}_1) w(t_2, t_1, \mathbf{n}'_2, \mathbf{n}'_1, \mathbf{k}) d\mathbf{n}_1 d\mathbf{n}'_1 d\mathbf{n}_2 d\mathbf{n}'_2 \right] \right\}, \quad (1) \end{aligned}$$

where

$$\begin{aligned} f(\mathbf{n}_{1,2}) &= \frac{e}{2\pi} \frac{\epsilon \mathbf{v}_{1,2}}{1 - \mathbf{n} \cdot \mathbf{v}_{1,2}}, \\ \mathbf{v}_{1,2} &= v \cdot \mathbf{n}_{1,2}, \quad \mathbf{n} = \frac{\mathbf{k}}{\omega}, \quad d\mathbf{n}_{1,2} \equiv d\omega_{1,2}, \quad T = \frac{L}{v}, \\ \nu(\mathbf{n}_2 - \mathbf{n}_1) &= \delta(\mathbf{n}_2 - \mathbf{n}_1) \int \sigma_0(\mathbf{n}'_2 - \mathbf{n}_1) d\mathbf{n}'_2 - \sigma_0(\mathbf{n}_2 - \mathbf{n}_1), \\ w(t_2, t_1, \mathbf{n}_2, \mathbf{n}_1, \mathbf{k}) &= \int \tilde{w}(t_2, t_1, \mathbf{r}_2 - \mathbf{r}_1, \mathbf{n}_2, \mathbf{n}_1) \times \\ & \quad \times \exp[i\omega(t_2 - t_1) - i\mathbf{k}(\mathbf{r}_2 - \mathbf{r}_1)] d\mathbf{r}_2. \end{aligned}$$

Here ϵ and \mathbf{k} are the polarization vector and the wave vector of the emitted photon; n_0 denotes the number of atoms in a unit volume of the medium; L is the thickness of the target; $\mathbf{n}_{1,2}$ are the unit vectors in the electron motion direction; \mathbf{v} and v are the electron velocity assumed to be invariant during the interaction with the target (the quantum-mechanical recoil effect is negligibly small) and its modulus; e is the electron charge; $\sigma_0(\mathbf{n}_2 - \mathbf{n}_1) = d\sigma/d\omega_{\mathbf{n}_2}$ presents the differential Born cross section of the electron scattering by target atoms, and $w(t_2, t_1, \mathbf{r}_2 - \mathbf{r}_1, \mathbf{n}_2, \mathbf{n}_1)$ is the electron distribution function in the coordinate \mathbf{r}_2 . The direction of motion \mathbf{n}_2 at time t_2 provided that at the time t_1 the electron had the coordinate \mathbf{r}_1 and moved in the direction characterized by the unit vector \mathbf{n}_1 .

The electron distribution function satisfies the kinetic equation

$$\begin{aligned} \frac{\partial w(t_2, t_1, \mathbf{r}_2 - \mathbf{r}_1, \mathbf{n}_2, \mathbf{n}_1)}{\partial t_2} &= -\mathbf{v}_2 \cdot \nabla_{\mathbf{r}_2} w(t_2, t_1, \mathbf{r}_2 - \mathbf{r}_1, \mathbf{n}_2, \mathbf{n}_1) - \\ & - n_0 \int \nu(\mathbf{n}_2 - \mathbf{n}'_1) \tilde{w}(t_2, t_1, \mathbf{r}_2 - \mathbf{r}_1, \mathbf{n}'_2, \mathbf{n}_1) d\mathbf{n}'_2 \quad (2) \end{aligned}$$

with the boundary condition

$$\tilde{w}(t_2, t_1, \mathbf{r}_2 - \mathbf{r}_1, \mathbf{n}_2, \mathbf{n}_1)|_{t_2=t_1} = \delta(\mathbf{r}_2 - \mathbf{r}_1) \delta(\mathbf{n}_2 - \mathbf{n}_1). \quad (3)$$

The term in (1) linear in n_0 is a ‘usual’ (incoherent) contribution to the intensity of the electron bremsstrahlung in the medium, derived by summation of the radiation intensities of the electron interaction with separate atoms of the target. The term quadratic in n_0 includes the contribution from the interference of the bremsstrahlung amplitudes on various atoms. The destructive character of this interference leads to suppression of the soft radiation intensity, i.e., to the Landau–Pomeranchuk effect.

For ω larger than $\omega_{\text{cr}} = 4\pi\gamma^2/(e^2L_R)$, where γ is the Lorentz factor of the scattered particle and L_R is the radiation length of the target material (for estimation of ω_{cr} , see [1, 2, 22]), the interference term becomes negligibly small, and radiation is of pure incoherent character.

1.2. Small-Angle Approximation. For ultrarelativistic particles ($1-v \ll 1$) it is convenient to pass in (1) to the small-angle approximation ($\vartheta_{1,2} \ll 1$) according to the scheme

$$\begin{aligned}\mathbf{n}_{1,2} &= \left(1 - \frac{\vartheta_{1,2}^2}{2}\right)\mathbf{n} + \boldsymbol{\vartheta}_{1,2}, & d\mathbf{n}_{1,2} &= d\boldsymbol{\vartheta}_{1,2}; \\ f(\mathbf{n}_{1,2}) &= f(\boldsymbol{\vartheta}_{1,2}) = \frac{e}{\pi} \frac{\boldsymbol{\epsilon} \boldsymbol{\vartheta}_{1,2}}{\vartheta_{1,2}^2 + \lambda^2}, & \lambda &= \frac{m}{E} = \gamma^{-1}; \\ \sigma_0(\mathbf{n}_2 - \mathbf{n}_1) &= \sigma_0(\boldsymbol{\vartheta}_2 - \boldsymbol{\vartheta}_1), & \delta(\mathbf{n}_2 - \mathbf{n}_1) &= \delta(\boldsymbol{\vartheta}_2 - \boldsymbol{\vartheta}_1), \\ \nu(\mathbf{n}_2 - \mathbf{n}_1) &= \nu(\boldsymbol{\vartheta}_2 - \boldsymbol{\vartheta}_1), & \boldsymbol{\vartheta}_2 - \boldsymbol{\vartheta}_1 &= \boldsymbol{\theta}; \\ w(t_2, t_1, \mathbf{n}_2, \mathbf{n}_1, \mathbf{k}) &= w(t_2, t_1, \boldsymbol{\vartheta}_2, \boldsymbol{\vartheta}_1, \omega)\end{aligned}\tag{4}$$

and further to the Fourier transforms of f, ν, w

$$\begin{aligned}f(\boldsymbol{\eta}) &= \frac{1}{2\pi} \int \tilde{f}(\boldsymbol{\theta}) \exp[i\boldsymbol{\eta}\boldsymbol{\theta}] d\boldsymbol{\theta} = \frac{ie\lambda\boldsymbol{\epsilon}\boldsymbol{\eta}}{\pi\eta} K_1(\lambda\eta), \\ \nu(\boldsymbol{\eta}) &= \int \tilde{\nu}(\boldsymbol{\theta}) e^{i\boldsymbol{\eta}\boldsymbol{\theta}} d\boldsymbol{\theta} = 2\pi \int \sigma_0(\boldsymbol{\theta}) [1 - J_0(\eta\theta)] \boldsymbol{\theta} d\boldsymbol{\theta},\end{aligned}\tag{5}$$

$$\begin{aligned}w(t_2, t_1, \boldsymbol{\eta}_2, \boldsymbol{\eta}_1, \omega) &= \frac{1}{(2\pi)^2} \int \tilde{w}(t_2, t_1, \boldsymbol{\vartheta}_2, \boldsymbol{\vartheta}_1, \omega) \times \\ &\quad \times \exp[i\boldsymbol{\eta}_2\boldsymbol{\vartheta}_2 - i\boldsymbol{\eta}_1\boldsymbol{\vartheta}_1] d\boldsymbol{\vartheta}_1 d\boldsymbol{\vartheta}_2,\end{aligned}$$

where $\boldsymbol{\vartheta}_{1(2)}$ denotes a two-dimensional electron scattering angle in the plane orthogonal to the electron direction at instant of time $t_{1(2)}$; m and E are the electron mass and its energy; $\boldsymbol{\theta}$ presents the electron multiple scattering angle over the time interval $t_2 - t_1$; λ is the characteristic frequency of the emitted photon; J_0 and K_1 are the Bessel and Macdonald functions, respectively.

Consequently, expression (1) is reduced to

$$\begin{aligned} \left\langle \frac{dI}{d\omega} \right\rangle = & \frac{2\lambda^2 e^2}{\pi^2} \left\{ n_0 L \int K_1^2(\lambda\eta) \nu(\eta) d\eta - \right. \\ & - n_0^2 \int_0^L dt_1 \int_0^L dt_2 \int \frac{(\boldsymbol{\eta}_1 \boldsymbol{\eta}_2)}{\eta_1 \eta_2} K_1(\lambda\eta_1) K_1(\lambda\eta_2) \nu(\eta_1) \nu(\eta_2) \times \\ & \left. \times \operatorname{Re} [w(t_2, t_1, \boldsymbol{\eta}_2, \boldsymbol{\eta}_1, \omega)] d\boldsymbol{\eta}_1 d\boldsymbol{\eta}_2 \right\}, \quad (6) \end{aligned}$$

where w satisfies the kinetic equation

$$\begin{aligned} \frac{\partial w(t_2, t_1, \boldsymbol{\eta}_2, \boldsymbol{\eta}_1, \omega)}{\partial t_2} = & \frac{i\omega}{2} (\lambda^2 - \Delta_{\boldsymbol{\eta}_2}) w(t_2, t_1, \boldsymbol{\eta}_2, \boldsymbol{\eta}_1, \omega) - \\ & - n_0 \nu(\eta_2) w(t_2, t_1, \boldsymbol{\eta}_2, \boldsymbol{\eta}_1, \omega) \quad (7) \end{aligned}$$

or, equivalently,

$$i \frac{\partial w(t_2, t_1, \boldsymbol{\eta}_2, \boldsymbol{\eta}_1, \omega)}{\partial t_2} = \left[\frac{\omega}{2} \Delta_{\boldsymbol{\eta}_2} - \frac{\omega}{2} \lambda^2 - i n_0 \nu(\eta_2) \right] w(t_2, t_1, \boldsymbol{\eta}_2, \boldsymbol{\eta}_1, \omega) \quad (8)$$

with the boundary condition

$$w(t_2, t_1, \boldsymbol{\eta}_2, \boldsymbol{\eta}_1, \omega) = \delta(\boldsymbol{\eta}_2 - \boldsymbol{\eta}_1). \quad (9)$$

The form of (8) is similar to the equation for Green's function of the two-dimensional Schrödinger equation with the mass ω^{-1} and the complex potential

$$U(\eta) = -\frac{\omega \lambda^2}{2} - i n_0 \nu(\eta) \quad (10)$$

and therefore admits of a formal solution in the form of a continual integral (see, e.g., [24]).

2. MULTIPLE SCATTERING THEORY

The theory of the multiple scattering of charged particles has been treated by several authors. However, most widespread at present is the multiple scattering theory of Molière [21]. The results of this theory are employed nowadays in most of the transport codes. It is of interest for numerous applications related to particle transport in matter, and it also presents the most used tool for taking into account the multiple scattering effects in experimental data processing.

As the Molière theory is currently used roughly for 10–300 GeV electron beams, the role of the high-energy corrections to the parameters of this theory becomes significant. Of special importance is the Coulomb correction to the screening angular parameter, as this parameter also enters into other important quantities in the Molière theory.

2.1. Molière's Theory of Multiple Scattering. Let $w_M(\vartheta, L)$ be a spatial-angle particle distribution function in a homogenous medium, and ϑ is a two-dimensional particle scattering angle in the plane orthogonal to the incident particle direction. For small-angle approximation $\vartheta \ll 1$ ($\sin \vartheta \sim \vartheta$), the above distribution function is the number of particles scattered in the angular interval $d\vartheta$ after traveling through the target of thickness L . In the notation of Molière, it reads

$$w_M(\vartheta, L) = \int_0^{\infty} J_0(\vartheta\eta) \exp[-n_0 L \nu(\eta)] \eta d\eta, \quad (11)$$

where

$$\nu(\eta) = 2\pi \int_0^{\infty} \sigma_0(\boldsymbol{\theta}) [1 - J_0(\theta\eta)] \boldsymbol{\theta} d\boldsymbol{\theta}. \quad (12)$$

The function (11) satisfies the well-known Boltzmann transport equation, written here with the small-angle approximation

$$\begin{aligned} \frac{\partial w(\vartheta, L)}{\partial L} &= -n_0 w_M(\vartheta, L) \int \sigma_0(\boldsymbol{\theta}) d^2\boldsymbol{\theta} + n_0 \int w_M(\boldsymbol{\vartheta} + \boldsymbol{\theta}, L) \sigma_0(\boldsymbol{\theta}) d^2\boldsymbol{\theta} = \\ &= n_0 \int [w_M(\boldsymbol{\vartheta} + \boldsymbol{\theta}, L) - w_M(\vartheta, L)] \sigma_0(\boldsymbol{\theta}) d^2\boldsymbol{\theta}. \end{aligned} \quad (13)$$

The Gaussian particle distribution function used in the Migdal LPM effect theory, which differs from (11), can be derived from the Boltzmann transport equation by the method of Fokker and Planck [26].

One of the most important results of the Molière theory is that the scattering is described by a single parameter, the so-called screening angle (θ_a or θ'_a)

$$\theta'_a = \sqrt{1.167} \theta_a = [\exp(C_E - 0.5)] \theta_a \approx 1.080 \theta_a, \quad (14)$$

where $C_E = 0.577\dots$ is the Euler constant.

More precisely, the angular distribution depends only on the logarithmic ratio b ,

$$b = \ln \left(\frac{\theta_c}{\theta'_a} \right)^2 \equiv \ln \left(\frac{\theta_c}{\theta_a} \right)^2 + 1 - 2C_E, \quad (15)$$

of the characteristic angle θ_c describing the foil thickness

$$\theta_c^2 = 4\pi n_0 L \left(\frac{Z\alpha}{\beta p} \right)^2, \quad p = mv, \quad (16)$$

to the screening angle θ'_a , which characterizes the scattering atom.

In order to obtain a result valid for large angles, Molière defines a new parameter B by the transcendental equation

$$B - \ln B = b. \quad (17)$$

The angular distribution function can then be written as

$$w_M(\vartheta, B) = \frac{1}{\vartheta^2} \int_0^\infty y dy J_0(\vartheta y) e^{-y^2/4} \exp\left[\frac{y^2}{4B} \ln\left(\frac{y^2}{4}\right)\right], \quad y = \theta_c \eta. \quad (18)$$

The Molière expansion method is to consider the term $y^2 \ln(y^2/4)/4B$ as a small parameter. Then, the angular distribution function is expanded in a power series in $1/B$:

$$w_M(\vartheta, L) = \sum_{n=0}^{\infty} \frac{1}{n!} \frac{1}{B^n} w_n(\vartheta, L), \quad (19)$$

in which

$$w_n(\vartheta, L) = \frac{1}{\vartheta^2} \int_0^\infty y dy J_0\left(\frac{\vartheta}{\vartheta} y\right) e^{-y^2/4} \left[\frac{y^2}{4} \ln\left(\frac{y^2}{4}\right)\right]^n, \quad (20)$$

$$\overline{\vartheta^2} = \theta_c^2 B = 4\pi n_0 L \left(\frac{Z\alpha}{\beta p}\right)^2 B(L). \quad (21)$$

This method is valid for $B \geq 4.5$ and $\overline{\vartheta^2} < 1$.

The first function $w_0(\vartheta, L)$ has a simple analytical form

$$w_0(\vartheta, L) = \frac{2}{\overline{\vartheta^2}} \exp\left(-\frac{\vartheta^2}{\overline{\vartheta^2}}\right), \quad (22)$$

$$\overline{\vartheta^2} \underset{L \rightarrow \infty}{\sim} \frac{L}{L_R} \ln\left(\frac{L}{L_R}\right). \quad (23)$$

For small angles, i.e., $\vartheta/\overline{\vartheta} = \vartheta/(\theta_c \sqrt{B})$ less than about 2, the Gaussian (22) is the dominant term. In this region, $w_1(\vartheta, L)$ is in general less than $w_0(\vartheta, L)$, so that the correction to the Gaussian is of order of $1/B$, i.e., about 10%.

A good approximate representation of the distribution at any angle is

$$w_M(\vartheta, L) = w_0(\vartheta, L) + \frac{1}{B} w_1(\vartheta, L) \quad (24)$$

with

$$w_1(\vartheta, L) = \frac{2}{\overline{\vartheta^2}} \exp\left(-\frac{\vartheta^2}{\overline{\vartheta^2}}\right) \left\{ \left(\frac{\vartheta^2}{\overline{\vartheta^2}} - 1\right) \left[\overline{Ei}\left(\frac{\vartheta^2}{\overline{\vartheta^2}}\right) - \ln\left(\frac{\vartheta^2}{\overline{\vartheta^2}}\right) \right] + 1 \right\} - 2, \quad (25)$$

$$\overline{Ei}(\Theta) = Ei(\Theta) + \pi i, \quad (26)$$

$$Ei(\Theta) = - \int_{-\Theta}^{\infty} e^{-L} \frac{dL}{L},$$

where $Ei(\Theta)$ is the exponential integral [27] and $\Theta = \vartheta^2/\vartheta'^2$. This approximation was applied by the authors of [23] to the analysis of data [15,16] over the region $\omega < 30$ MeV that will be shown in Sec. 3.

Let us notice that the expression (12) for the function $\nu(\eta)$ is identical to (5). As was shown in classical works of Molière [21], this quantity can be represented in the area of the important η values $0 \leq \eta \leq 1/\theta_c$ as

$$\nu(\eta) = -4\pi \left(\frac{Z\alpha}{\beta p} \right)^2 \eta^2 \left[\ln \left(\frac{\eta \theta_a}{2} \right) + C_E - \frac{1}{2} \right], \quad (27)$$

where the screening angle θ_a depends both on the screening properties of the atom and on the σ_0 approximation used for its calculation.

Using the Thomas–Fermi model of the atom and an interpolation scheme, Molière obtained θ_a for the cases where σ_0 is calculated within the Born and quasi-classical approximations:

$$\theta_a^B = 1.20 \alpha Z^{1/3}, \quad (28)$$

$$\theta_a = \theta_a^B \sqrt{1 + 3.34 (Z\alpha/\beta)^2}. \quad (29)$$

The latter result is only approximate (see critical remarks on its derivation in [26]). Below we will present an exact analytical and numerical result for this angular parameter.

2.2. Coulomb Correction to the Screening Angular Parameter. Recently, it has been shown [20] by means of [6] that for any model of the atom the following rigorous relation determining the screening angular parameter θ'_a is valid:

$$\ln(\theta'_a) = \ln(\theta_a^B) + \text{Re} [\psi(1 + iZ\alpha/\beta)] + C_E$$

or, equivalently,

$$\Delta_{CC}[\ln(\theta'_a)] \equiv \ln(\theta'_a) - \ln(\theta_a^B) = f(Z\alpha/\beta), \quad (30)$$

where Δ_{CC} is the so-called Coulomb correction to the Born result, ψ is the logarithmic derivative of the gamma function Γ , and $f(Z\alpha/\beta)$ is a universal function of the Born parameter $\xi = Z\alpha/\beta$ which is also known as the Bethe–Maximon function:

$$f(\xi) = \xi^2 \sum_{n=1}^{\infty} \frac{1}{n(n^2 + \xi^2)}. \quad (31)$$

To compare the approximate Molière result (29) with the exact one (30), we first present (29) in the form

$$\delta_M \equiv \frac{\theta_a - \theta_a^B}{\theta_a^B} = \sqrt{1 + 3.34 (Z\alpha/\beta)^2} - 1 \quad (32)$$

and also rewrite (30) as follows:

$$\delta_{CC} \equiv \frac{\theta_a - \theta_a^B}{\theta_a^B} = \frac{\theta'_a - (\theta'_a)^B}{(\theta'_a)^B} = \exp[f(\xi)] - 1. \quad (33)$$

Then we get

$$\delta_{MCC} \equiv \frac{\delta_M - \delta_{CC}}{\delta_M} = \frac{\Delta_{MCC}}{\delta_M}. \quad (34)$$

For some targets used in [15, 16] and $\beta = 1$, we have obtained the following values of relative Molière δ_M and Coulomb δ_{CC} corrections and also values of the difference Δ_{MCC} and relative difference δ_{MCC} between the approximate Molière (32) and exact (33) results (Table 1).

Table 1. The difference between the approximate (32) and exact (33) results for the Coulomb correction to the screening angle

Target	Z	$\delta_M, \%$	$\delta_{CC}, \%$	$\Delta_{MCC}, \%$	$\delta_{MCC}, \%$
W	74	40.4	32.5	7.5	19.6
Pt	78	44.3	35.9	8.4	19.0
Au	79	45.2	36.7	8.5	18.8
Pb	82	48.2	39.3	8.9	18.5
U	92	58.3	48.5	9.8	16.9

For instance, Table 1 shows that the difference and relative difference between the approximate and exact results for these Coulomb correction reach 8.5% and 18.8%, respectively, in the case of the gold target discussed in [8, 15, 16].

We show further that the above discrepancy between theory and experiment [8, 15, 16] can be completely eliminated on the basis of these Coulomb corrections to the screening angular parameter.

3. COULOMB CORRECTIONS IN THE LPM EFFECT THEORY AND ITS ANALOGUE FOR A THIN LAYER OF MATTER

3.1. Coulomb Corrections to the Parameters of the Migdal LPM Effect Theory. The analytical solution of Eq.(7) with arbitrary values of ω is only possible within the Fokker–Planck approximation*

$$\nu(\eta) = a\eta^2, \quad (35)$$

*An explicit expression for w obtained in this approach can be found in [4].

but at $\omega = 0$ it is also possible for arbitrary $\nu(\eta)$.

In the latter case ($\omega = 0$)

$$w(t_2, t_1, \boldsymbol{\eta}_2, \boldsymbol{\eta}_1, 0) = \delta(\boldsymbol{\eta}_2 - \boldsymbol{\eta}_1) \exp[-n_0 \nu(\eta_2)(t_2 - t_1)], \quad (36)$$

and integration over t_1, t_2 in (6) is carried out trivially, leading to the simple result

$$\left\langle \frac{dI}{d\omega} \right\rangle \Big|_{\omega=0} = \frac{4\lambda^2 e^2}{\pi} \int K_1^2(\lambda\eta) \{1 - \exp[-n_0 L \nu(\eta)]\} \eta d\eta. \quad (37)$$

Considering the aforesaid, in the other limiting case ($\omega \gg \omega_{\text{cr}}$) we get

$$\left\langle \frac{dI}{d\omega} \right\rangle \Big|_{\omega \gg \omega_{\text{cr}}} = n_0 L \lambda^2 e^2 \int K_1^2(\lambda\eta) \nu(\eta) \eta d\eta. \quad (38)$$

3.1.1. Case $\omega \gg \omega_{\text{cr}}$. After the substitution of $\nu(\eta)$ (27) into (38), the integration is carried out analytically, leading to the following result:

$$\left\langle \frac{dI}{d\omega} \right\rangle \Big|_{\omega \gg \omega_{\text{cr}}} = \frac{16}{3\pi} \frac{Z^2 \alpha^3}{m^2} \left(\ln \frac{\lambda}{\theta_a} + \frac{7}{12} \right) n_0 L. \quad (39)$$

Let us find an analytical expression for the Coulomb correction to the Born spectral bremsstrahlung rate (39):

$$\begin{aligned} \Delta_{\text{CC}}[\langle dI/d\omega \rangle] &\equiv \left\langle \frac{dI}{d\omega} \right\rangle - \left\langle \frac{dI}{d\omega} \right\rangle^{\text{B}} = \\ &= -\frac{16 Z^2 \alpha^3 n_0 L}{3\pi m^2} \left[\ln(\theta'_a) - \ln(\theta'_a)^{\text{B}} \right] = -\frac{16 Z^2 \alpha^3 n_0 L}{3\pi m^2} f(\xi). \end{aligned} \quad (40)$$

Then, the corresponding relative Coulomb correction reads

$$\delta_{\text{CC}}[\langle dI/d\omega \rangle] \equiv \frac{\langle dI/d\omega \rangle - \langle dI/d\omega \rangle^{\text{B}}}{\langle dI/d\omega \rangle^{\text{B}}} = -\frac{f(\xi)}{0.583 - \ln(1.2 \alpha Z^{1/3})}. \quad (41)$$

Let us enter the ratio

$$R_{\text{CC}}(\omega) = \frac{\langle dI(\omega)/d\omega \rangle}{\langle dI(\omega)/d\omega \rangle^{\text{B}}} = \delta_{\text{CC}}[\langle dI/d\omega \rangle] + 1. \quad (42)$$

We will also estimate the numerical values of (41) and (42) for $\beta = 1$ (Table 2). It is seen from Table 2 that the relative correction to the Born spectral bremsstrahlung rate $\delta_{\text{CC}}[\langle dI/d\omega \rangle]$ is about -8% and the corresponding ratio $R(\omega)|_{\omega \gg \omega_{\text{cr}}}$ is approximately 0.92 for the gold target discussed in [15]*.

*The use of approximate Molière's result (29) for θ_a would give the value $R(\omega)|_{\omega \gg \omega_{\text{cr}}} = 0.900$ in the discussed case.

Table 2. The relative Coulomb correction $\delta_{CC}[\langle dI/d\omega \rangle]$ to the Born spectral bremsstrahlung rate for $\omega \gg \omega_{cr}$ and $\beta = 1$

Target	Z	$Z\alpha$	$f(Z\alpha)$	$-\delta_{CC}$	R_{CC}
Be	4	0.029	0.001	0.000	1.000
C	6	0.044	0.004	0.001	0.999
Al	13	0.094	0.011	0.002	0.998
Ti	22	0.160	0.031	0.007	0.993
Fe	26	0.190	0.043	0.010	0.990
Ni	28	0.204	0.049	0.012	0.988
Mo	42	0.307	0.105	0.026	0.974
Sn	50	0.365	0.144	0.036	0.964
Ta	73	0.533	0.276	0.071	0.929
W	74	0.540	0.281	0.072	0.928
Pt	78	0.569	0.307	0.079	0.921
Au	79	0.577	0.312	0.081	0.919
Pb	82	0.598	0.332	0.086	0.914
U	92	0.671	0.395	0.104	0.896

3.2. Case $\omega = 0$. In the other limiting case the performance of numerical integration in (37) get the following results for the relative Coulomb correction $-\delta_{CC}[\langle dI/d\omega \rangle]$ and the ratio $R(\omega)|_{\omega=0}$ (Table 3) at thicknesses of experimental targets $L = 0.7-6\%L_R$ [15]. Here $L_R \approx 0.33$ cm is the radiation length of the target material ($Z = 79$)

$$L_R = \frac{4Z^2 e^6 n_0}{m^2} \ln(183Z^{1/3}). \quad (43)$$

Table 3. The relative correction $\delta_{CC}[\langle dI/d\omega \rangle]$ for $Z = 79$ and $\omega = 0$

L , cm	$-\delta_{CC}$	R_{CC}	L , cm	$-\delta_{CC}$	R_{CC}
$0.007 L_R$	0.039	0.961	$0.060 L_R$	0.018	0.982

3.3. Case $\omega_{cr} > \omega$. When $\omega_{cr} > \omega > 0$, it is obvious from general considerations that

$$R_{CC}(\omega)|_{\omega > \omega_{cr}} \leq R_{CC}(\omega)|_{\omega_{cr} > \omega} \leq R_{CC}(\omega)|_{\omega=0}. \quad (44)$$

From Table 3 and (44) it follows that the calculation results for $\langle dI/d\omega \rangle$ cannot be obtained from the Born approximation results by multiplying them by the normalization constant, which is independent of the frequency ω and target thickness L .

However, considering a nearly 3.2% systematic error of the experimental data [15] in the range $500 > \omega > 30$ MeV, it is clear why multiplication by the normalization factor helped the authors [8, 15, 16] to get reasonable agreement of the Born calculation results with the experimental data.

Considering the two previous limiting cases allows one to obtain some interpolation values for $R_{CC}(\omega)|_{\omega_{cr} > \omega}$ from Tables 2 and 3 (see Table 4).

Table 4. The interpolation values of the ratio $R_{CC}(\omega, L)$ for $\omega < \omega_{cr}$, $Z = 79$, and $\beta = 1$

L , cm	$R_{CC}(\omega, L)$	$\bar{R}_{CC}(\omega) _{\omega < \omega_{cr}}$
$0.007 L_R$	$0.920 \leq R_{CC}(\omega) _{\omega < \omega_{cr}} \leq 0.961$	0.940
$0.060 L_R$	$0.920 \leq R_{CC}(\omega) _{\omega < \omega_{cr}} \leq 0.982$	0.951

So for target thicknesses $0.007 L_R$ to $0.060 L_R$, the averaged value of the ratio $R_{CC}(\omega, L)|_{\omega < \omega_{cr}}$ is approximately 0.945 ± 0.008 , which coincides within the experimental error with the normalization factor value $0.94 \pm 0.01 \pm 0.032$ introduced in [15] for obtaining agreement of the calculations performed in the Born approximation with experiment. The obtained result means that the normalization is not required for $\langle dI(\omega)/d\omega \rangle$ calculated on the basis of the refined screening angle.

We will now obtain the analytical expressions and numerical estimations for the Coulomb corrections to the function $\nu(\eta) = 2\pi \int \sigma_0(\theta)[1 - J_0(\eta\theta)]\theta d\theta$ (5) and the complex potential $U(\eta) = -\omega\lambda^2/2 - i n_0\nu(\eta)$ (35).

For the first quantity, using (27), we obtain

$$\begin{aligned} \Delta_{CC}[\nu(\eta)] &\equiv \nu(\eta) - \nu^B(\eta) = \\ &= -4\pi\eta^2 \left(\frac{Z\alpha}{\beta p} \right)^2 \Delta_{CC}[\ln(\theta'_a)] = -4\pi\eta^2 \left(\frac{Z\alpha}{\beta p} \right)^2 f(\xi). \end{aligned} \quad (45)$$

The Coulomb correction to the potential (35) becomes

$$\Delta_{CC}[U(\eta)] \equiv U(\eta) - U^B(\eta) = -4\pi i n_0 \eta^2 \left(\frac{Z\alpha}{\beta p} \right)^2 f(\xi). \quad (46)$$

Now we obtain the corresponding relative Coulomb corrections. Using (5), we get

$$\delta_{CC}[U(\eta)] \equiv \frac{\Delta_{CC}[U(\eta)]}{U^B(\eta)} = \frac{\Delta_{CC}[\nu(\eta)]}{\nu^B(\eta)} \equiv \delta_{CC}[\nu(\eta)]. \quad (47)$$

Then (27), (28), and (45) give

$$\delta_{CC}[\nu(\eta)] = \frac{f(Z\alpha/\beta)}{\ln \eta + \ln(\theta_a^B) - \ln 2 + C_E - 0.5} = \quad (48)$$

$$= -\frac{f(Z\alpha/\beta)}{0.615 - \ln(1.2\alpha Z^{1/3}) - \ln \eta}. \quad (49)$$

We see from (48) and (41) that

$$\delta_{\text{CC}}[\nu(\eta)] = \delta_{\text{CC}}[U(\eta)] < \delta_{\text{CC}}[\langle dI/d\omega \rangle], \quad (50)$$

and we can estimate the $\delta_{\text{CC}}[\nu(\eta)]$ values from (48) for $\eta \ll 1$. Their numerical values are presented in Table 5.

Table 5. The relative Coulomb corrections $\delta_{\text{CC}}[\nu(\eta)]$ and $\delta_{\text{CC}}[U(\eta)]$ for the gold, lead, and uranium targets

Z	$a \leq \eta \leq b$	$-\delta_{\text{CC}}[\nu(\eta)] = -\delta_{\text{CC}}[U(\eta)]$
79	$0.01 \leq \eta \leq 0.1$	$3.7\% \leq -\delta_{\text{CC}}[\nu(\eta)] \leq 5.0\%$
82	$0.01 \leq \eta \leq 0.1$	$3.9\% \leq -\delta_{\text{CC}}[\nu(\eta)] \leq 5.3\%$
92	$0.01 \leq \eta \leq 0.1$	$5.5\% \leq -\delta_{\text{CC}}[\nu(\eta)] \leq 8.0\%$

Thus, for instance, $-\delta_{\text{CC}}[\nu(\eta)] = -\delta_{\text{CC}}[U(\eta)] \sim 4.3\% < -\delta_{\text{CC}}[\langle dI/d\omega \rangle] \sim 8.0\%$ for $Z = 79$ (Au).

Let us consider the spectral bremsstrahlung intensity (6) in the form proposed by Migdal:

$$\left\langle \frac{dI}{d\omega} \right\rangle = \Phi(s) \left(\frac{dI}{d\omega} \right)_0, \quad (51)$$

where $(dI/d\omega)_0$ is the spectral bremsstrahlung rate without accounting for the multiple scattering effects in the radiation,

$$\left(\frac{dI}{d\omega} \right)_0 = \frac{2e^2}{3\pi} \gamma^2 q L, \quad (52)$$

$$q = \overline{v^2}/L. \quad (53)$$

The function $\Phi(s)$ in (51) accounts for the multiple scattering influence on the bremsstrahlung rate,

$$\Phi(s) = 24s^2 \left[\int_0^\infty dx e^{-2sx} \text{cth}(x) \sin(2sx) - \frac{\pi}{4} \right], \quad (54)$$

$$s^2 = \lambda^2 / \overline{v^2}. \quad (55)$$

It has simple asymptotes at the small and large values of the argument:

$$\Phi(s) \approx \begin{cases} 1, & s > 1, \\ 6s, & s \ll 1, \end{cases} \quad (56)$$

$$s = \frac{1}{4\gamma^2} \sqrt{\frac{\omega}{q}}. \quad (57)$$

The formula (51) is obtained with the logarithmic accuracy. At $s > 1$, (51) coincides to the logarithmic accuracy with the Bethe–Heitler result

$$\left\langle \frac{dI}{d\omega} \right\rangle_{\text{BH}} = \frac{L}{L_R} \left[1 + \frac{1}{12 \ln(183Z^{-1/3})} \right]. \quad (58)$$

If $s \ll 1$, we have the suppression of the spectral density of radiation in comparison with (58).

Now we obtain analytical and numerical results for the Coulomb corrections to these quantities. In order to derive an analytical expression for the Coulomb correction to the Born spectral bremsstrahlung rate $(dI/d\omega)_0$, we first write

$$\Delta_{\text{CC}} \left[\left(\frac{dI}{d\omega} \right)_0 \right] \equiv \left(\frac{dI}{d\omega} \right)_0 - \left(\frac{dI}{d\omega} \right)_0^B = \frac{2e^2}{3\pi} \gamma^2 L \Delta_{\text{CC}}[q], \quad (59)$$

$$\Delta_{\text{CC}}[q] \equiv q - q^B = \frac{1}{L} \Delta_{\text{CC}}[\overline{\vartheta^2}]. \quad (60)$$

Accounting for $\overline{\vartheta^2} = \theta_c^2 B$ (21), we get

$$\Delta_{\text{CC}}[\overline{\vartheta^2}] \equiv \overline{\vartheta^2} - \left(\overline{\vartheta^2} \right)^B = \theta_c^2 \Delta_{\text{CC}}[B]. \quad (61)$$

Then, using (15) and (90), we arrive at

$$\Delta_{\text{CC}}[b] = -f(\xi) = \left(1 - \frac{1}{B^B} \right) \Delta_{\text{CC}}[B], \quad (62)$$

$$\Delta_{\text{CC}}[B] = \frac{f(\xi)}{1/B^B - 1}. \quad (63)$$

Finally, (59) becomes

$$\Delta_{\text{CC}} \left[\left(\frac{dI}{d\omega} \right)_0 \right] = \frac{2(e\gamma\theta_c)^2}{3\pi(1/B^B - 1)} f(\xi), \quad (64)$$

and the relative Coulomb correction reads

$$\begin{aligned} \delta_{\text{CC}} [(dI/d\omega)_0] &= \delta_{\text{CC}}[q] = \delta_{\text{CC}}[\overline{\vartheta^2}] = \delta_{\text{CC}}[B] = \\ &= R_{\text{CC}} [(dI/d\omega)_0] - 1 = \frac{f(\xi)}{1 - B^B}. \end{aligned} \quad (65)$$

Next, in order to obtain the relative Coulomb correction to the Migdal function $\Phi(s)$, we first derive corresponding correction to the quantity s^2 (55):

$$\Delta_{\text{CC}}[s^2] = \frac{\omega}{16\gamma^4} \left(\frac{1}{q} - \frac{1}{q^B} \right), \quad (66)$$

$$\delta_{\text{CC}} [s^2] = \frac{q^B}{q} - 1 = \frac{(\overline{\vartheta^2})^B}{\overline{\vartheta^2}} - 1, \quad (67)$$

where

$$(\overline{\vartheta^2})^B / \overline{\vartheta^2} = \left(\delta_{\text{CC}} [\overline{\vartheta^2}] + 1 \right)^{-1}. \quad (68)$$

This leads to the following relative Coulomb correction for s (57):

$$\delta_{\text{CC}} [s] = \left((\overline{\vartheta^2})^B / \overline{\vartheta^2} \right)^{1/2} - 1 = \left(\delta_{\text{CC}} [\overline{\vartheta^2}] + 1 \right)^{-1/2} - 1. \quad (69)$$

For the asymptote $\Phi(s) = 6s$ (56), we get

$$\delta_{\text{CC}} [\Phi(s)] = \delta_{\text{CC}} [s] = \left(R_{\text{CC}} [(dI/d\omega)_0] \right)^{-1/2} - 1. \quad (70)$$

Then, the total relative Coulomb correction to $\langle dI/d\omega \rangle$ in this asymptotic case becomes

$$\delta_{\text{CC}} [\langle dI/d\omega \rangle] = \delta_{\text{CC}} [(dI/d\omega)_0] + \delta_{\text{CC}} [\Phi(s)]. \quad (71)$$

Numerical values of these corrections for some specified values of the Molière parameter B^B are presented in Table 6.

As can be seen from Table 6, the moduli of the Coulomb corrections to the quantities $(dI/d\omega)_0^B$ and $\Phi^B(s)$ decrease from about 9 to 4% and from 5 to 2%, respectively, with an increase in the parameter B^B from a minimum value 4.5 [21] to a value 8.46 corresponding to the conditions of experiment [23]; and the modulus of the total relative correction $\delta_{\text{CC}} [\langle dI/d\omega \rangle]$ decreases from approximately 14 to 6%. Let us notice that the average value of the ratio $\bar{R}_{\text{CC}} = 0.947 \pm 0.015$ for the gold target coincides with the corresponding value $\bar{R}_{\text{CC}} = 0.945 \pm 0.008$ from Table 4. This corresponds to the mean value $\bar{\delta}_{\text{CC}} = -5.4\%$, which coincides with the value of the normalization correction $(-5.5 \pm 0.2)\%$ for $6\%L_R$ gold target (Table II in [16]).

A comparison of the non-averaged ratio value $R_{\text{CC}} [\langle dI/d\omega \rangle] = 0.936$ from Table 6 with the normalization factor $R \sim 0.94$ would be unjustified, because the regime of strong suppression ($s \ll 1$ and $\Phi(s) \approx 6s$) is not achieved in the analyzed SLAC experiment. For such a comparison, we will carry out now

Table 6. Relative Coulomb corrections to the parameters of the Migdal LPM theory, $\delta_{\text{CC}} [(dI/d\omega)_0]$ (65), $\delta_{\text{CC}} [\Phi(s)]$ (70), and $\delta_{\text{CC}} [\langle dI/d\omega \rangle]$ (71) for $Z = 79$ (Au) and $\beta = 1$

B^B	$\delta_{\text{CC}} \left[\left(\frac{dI}{d\omega} \right)_0 \right]$	$R_{\text{CC}} \left[\left(\frac{dI}{d\omega} \right)_0 \right]$	$\delta_{\text{CC}} [\Phi(s)]$	$\delta_{\text{CC}} \left[\left\langle \frac{dI}{d\omega} \right\rangle \right]$	$R_{\text{CC}} \left[\left\langle \frac{dI}{d\omega} \right\rangle \right]$
4.50	-0.089	0.911	-0.048	-0.137	0.863
4.90	-0.080	0.920	-0.043	-0.123	0.877
8.46	-0.042	0.958	-0.022	-0.064	0.936

calculation for the regime of small LPM suppression ($s \geq 1$ and $\Phi(s) \approx 1 - 0.012/s^4$).

In order to obtain the relative correction $\delta_{CC}[\Phi(s)]$ in this regime, we first derive an expression for the Coulomb correction $\Delta_{CC}[\Phi(s)]$ to the Migdal function $\Phi(s)$:

$$\Delta_{CC}[\Phi(s)] = 0.012 \left(\frac{1}{(s^4)^B} - \frac{1}{s^4} \right) = \frac{0.012}{s^4} \delta_{CC}[s^4], \quad (72)$$

$$\begin{aligned} \delta_{CC}[s^4] &= \left(\frac{q^B}{q} \right)^2 - 1 = \left(\frac{(\vartheta^2)^B}{\vartheta^2} \right)^2 - 1 = 1 / \left(\delta_{CC}[\vartheta^2] + 1 \right)^2 - 1 = \\ &= 1 / \left(R_{CC}[(dI/d\omega)_0] \right)^2 - 1. \end{aligned} \quad (73)$$

This leads to the following relative Coulomb correction for $\Phi(s)$:

$$\begin{aligned} \delta_{CC}[\Phi(s)] &= \frac{0.012}{s^4} \delta_{CC}[s^4] \frac{(s^4)^B}{(s^4)^B - 0.012} = \\ &= 0.012 \frac{\delta_{CC}[s^4]}{\delta_{CC}[s^4] + 1} \frac{1}{(s^4)^B - 0.012}. \end{aligned} \quad (74)$$

In Table 7 are listed the values of the relative Coulomb corrections to the quantities of (51) in the regime of small suppression for some separate s values ($s = 1.2$ and $s = 1.3$).

Table 8 presents the values of the corrections $-\delta_{CC}[\langle dI/d\omega \rangle]$ (%) for separate high- Z target elements over the entire range $1.0 \leq s \leq \infty$ of the parameter s ,

Table 7. Relative Coulomb corrections to the quantities of the Migdal LPM theory, $\delta_{CC}[(dI/d\omega)_0]$, $\delta_{CC}[\Phi(s)]$, and $\delta_{CC}[\langle dI/d\omega \rangle]$, in the regime of small LPM suppression for high- Z targets of experiment [16]

Target	Z	$\delta_{CC} \left[\left(\frac{dI}{d\omega} \right)_0 \right]$	$\delta_{CC}[s^4]$	$\delta_{CC}[\Phi(s)]$	$\delta_{CC} \left[\left\langle \frac{dI}{d\omega} \right\rangle \right]$	$R_{CC} \left[\left\langle \frac{dI}{d\omega} \right\rangle \right]$
1. For $\beta = 1$, $B^B = 8.46$, $s = 1.2$						
Au	79	-0.0420	-0.0896	-0.0006	-0.0426	0.9574
Pb	82	-0.0445	-0.0953	-0.0006	-0.0451	0.9549
U	92	-0.0529	-0.1149	-0.0007	-0.0536	0.9464
2. For $\beta = 1$, $B^B = 8.46$, $s = 1.3$						
Au	79	-0.0420	-0.0896	-0.0004	-0.0424	0.9576
Pb	82	-0.0445	-0.0953	-0.0004	-0.0449	0.9551
U	92	-0.0529	-0.1149	-0.0005	-0.0534	0.9466
<i>Note:</i>						
For case 1 $\bar{R}_{CC}[\langle dI/d\omega \rangle] = 0.953 \pm 0.006$; $\bar{\delta}_{CC}[\langle dI/d\omega \rangle] = (-4.71 \pm 0.58)\%$.						
For case 2 $\bar{R}_{CC}[\langle dI/d\omega \rangle] = 0.953 \pm 0.006$; $\bar{\delta}_{CC}[\langle dI/d\omega \rangle] = (-4.69 \pm 0.58)\%$.						

for which the regime of small LPM suppression is valid. It also gives the sampling mean of the corrections $-\bar{\delta}_{CC}[\langle dI/d\omega \rangle]$ (%) over the range $1.0 \leq s \leq \infty$.

Table 8. The dependence of $-\delta_{CC}[\langle dI/d\omega \rangle]$ values on the parameter s in the regime of small LPM suppression for some high- Z targets of experiment [16] at $\beta = 1$ and $B^B = 8.46$

Z	$s = 1.0$	$s = 1.1$	$s = 1.2$	$s = 1.3$	$s = 1.5$	$s = 2.0$	$s = \infty$
79	0.0432	0.0428	0.0426	0.0424	0.0422	0.0421	0.0420
82	0.0458	0.0454	0.0451	0.0449	0.0447	0.0446	0.0445
92	0.0545	0.0540	0.0536	0.0534	0.0532	0.0530	0.0529

Note:

$\delta_{CC}[\langle dI/d\omega \rangle] = (-4.50 \pm 0.05)\%$ ($Z = 82$),
$\delta_{CC}[\langle dI/d\omega \rangle] = (-5.35 \pm 0.06)\%$ ($Z = 92$),
$\bar{\delta}_{CC}[\langle dI/d\omega \rangle] = (-4.70 \pm 0.49)\%$.

Table 8 shows that averaging over the range $1.0 \leq s \leq \infty$ corrections $\delta_{CC}[\langle dI/d\omega \rangle]$ for some separate high- Z targets* gives their sampling means $\delta_{CC}[\langle dI/d\omega \rangle] = (-4.50 \pm 0.05)\%$ ($Z = 82$) and $\delta_{CC}[\langle dI/d\omega \rangle] = (-5.35 \pm 0.06)\%$ ($Z = 92$), which coincide with the normalization correction values $(-4.5 \pm 0.2)\%$ for $2\%L_R$ lead target and $(-5.6 \pm 0.3)\%$ for $3\%L_R$ uranium target (Table II in [16]), respectively, within the experimental error.

Averaging corrections $\bar{\delta}_{CC}[\langle dI/d\omega \rangle]$ over this range gives the sampling mean $(-4.70 \pm 0.49)\%$, which excellently agrees with the weighted average value $(-4.7 \pm 2)\%$ of the normalization correction obtained in [16] for 25 GeV data**. We believe that this allows one to understand the origin of the normalization problem for high- Z targets discussed in [15, 16].

3.4. Fokker–Planck Approximation Accuracy in the Case $\omega = 0$. Finally, let us briefly discuss the accuracy of the Fokker–Planck approximation that allows an analytical expression to be derived for the Migdal particle distribution function and entire $\langle dI(\omega)/d\omega \rangle$ range to be rather simply calculated (using numerical calculation of triple integrals).

To this end, we will fix the parameter a in expression (35) in such a way that the results of the exact calculation of $\langle dI(\omega)/d\omega \rangle|_{\omega \gg \omega_{cr}}$ and its calculation in the Fokker–Planck approximation coincide. As a result, we get

*For low- Z targets, the E-146 data showed a disagreement with the Migdal LPM theory predictions. There is a problem of an adequate description of the photon spectra shape for the low- Z targets [16]. Therefore, we will analyze only results for some high- Z targets of the SLAC E-146 experiment.

**It becomes $(-4.8 \pm 3.5)\%$ for the 8 GeV data if the outlying $6\%L_R$ gold target is excluded from them [16].

$$a = 2\pi \left(\frac{Z\alpha\sigma}{m} \right)^2 \left(\ln \frac{\sigma}{\theta_a} + \frac{7}{12} \right). \quad (75)$$

Now we calculate $\langle dI(\omega)/d\omega \rangle|_{\omega=0}$ using the relations (35) and (75) and compare the result with the result obtained using ‘realistic’ (Molière) expression (27) for $\nu(\eta)$. Then for the ratio

$$R_{\text{FPM}} = \frac{\langle dI(\omega)/d\omega \rangle_{\text{FP}}}{\langle dI(\omega)/d\omega \rangle_{\text{M}}} \quad (76)$$

we get the following values:

$$R_{\text{FPM}}(\omega, L) = \begin{cases} 0.890, & L = 0.007 L_R \\ 0.872, & L = 0.060 L_R \end{cases}. \quad (77)$$

The values of corresponding relative corrections

$$\delta_{\text{FPM}}[\langle dI/d\omega \rangle] = \frac{\langle dI(\omega)/d\omega \rangle_{\text{FP}} - \langle dI(\omega)/d\omega \rangle_{\text{M}}}{\langle dI(\omega)/d\omega \rangle_{\text{M}}} \quad (78)$$

in percentage are given in Table 9.

Table 9. The relative correction $\delta_{\text{FPM}}[\langle dI/d\omega \rangle]$ for $Z = 79$ and $\omega = 0$

L , cm	$-\delta_{\text{FPM}}$	R_{FPM}	L , cm	$-\delta_{\text{FPM}}$	R_{FPM}
$0.007 L_R$	0.110	0.890	$0.060 L_R$	0.128	0.872

It is obvious that the relative difference between the Fokker–Planck approximation and the description based on the Molière theory $\delta_{\text{FPM}}[\langle dI/d\omega \rangle]$ is about 12%, which is noticeably higher than the 3.2% characteristic systematic experimental error [15].

Thus, the Fokker–Planck approximation and Gaussian distribution cannot be used for describing the experimental data [15,16] at low frequencies $\omega < 30$ MeV. For their description the application of the Molière multiple scattering theory is advisable.

3.5. Coulomb Corrections in the LPM Effect Theory Analogue for a Thin Target. In [23] it is shown that the region of the emitted photon frequencies $\omega_{\text{cr}} > \omega > 0$ naturally splits into two intervals, $\omega_{\text{cr}} > \omega > \omega_c$ and $\omega_c > \omega > 0$, in the first of which the LPM effect for sufficiently thick targets takes place, and in the second, there is its analogue for thin targets. The quantity ω_c is defined here as $\omega_c = 2E^2/(m^2L)$.

Application of the Molière multiple scattering theory to the analysis of experimental data [15,16] for a thin target in the second ω range is based on the use of the expression for the spatial-angle particle distribution function (11) which satisfies the standard Boltzmann transport equation for a thin homogeneous foil, and it differs significantly from the Gaussian particle distribution of the Migdal LPM effect theory.

Besides, it determines another expression for the spectral radiation rate in the context of the coherent radiation theory [23], which reads

$$\left\langle \frac{dI}{d\omega} \right\rangle = \int w_M(\vartheta) \frac{dI(\vartheta)}{d\omega} d^2\vartheta. \quad (79)$$

Here

$$\frac{dI(\vartheta)}{d\omega} = \frac{2e^2}{\pi} \left[\frac{2\chi^2 + 1}{\chi\sqrt{\chi^2 + 1}} \ln(\chi + \sqrt{\chi^2 + 1}) - 1 \right] \quad (80)$$

with $\chi = \gamma\vartheta/2$. The latter expression is valid for consideration of the particle scattering in both amorphous and crystalline medium.

The formula (80) has simple asymptotes at the small and large values of parameter χ :

$$\frac{dI(\vartheta)}{d\omega} = \frac{2e^2}{3\pi} \begin{cases} \gamma^2\vartheta^2, & \gamma\vartheta \ll 1, \\ 3 [\ln(\gamma^2\vartheta^2) - 1], & \gamma\vartheta \gg 1, \end{cases} \quad (81)$$

Replacing in this formula ϑ^2 by the average square value of the scattering angle $\overline{\vartheta^2}$, we arrive at the following estimates for the average radiation spectral density value:

$$\left\langle \frac{dI}{d\omega} \right\rangle = \frac{2e^2}{3\pi} \begin{cases} \gamma^2\overline{\vartheta^2}, & \gamma^2\overline{\vartheta^2} \ll 1, \\ 3 [\ln(\gamma^2\overline{\vartheta^2}) - 1], & \gamma^2\overline{\vartheta^2} \gg 1. \end{cases} \quad (82)$$

In the experiment [15,16], the above frequency intervals correspond roughly to the following ω ranges: $(\omega_{cr} > \omega > \omega_c) \sim (350 \text{ MeV} > \omega > 30 \text{ MeV})$ and $(\omega_c > \omega > 0) \sim (30 \text{ MeV} > \omega > 5 \text{ MeV})$ for 25 GeV electron beam and 0.7–6.0% L_R gold target. Whereas in the first area the discrepancy between the LPM theory predictions and data is about 3.2 to 5% which requires the use of normalization factor $R \sim 0.94$, in the second area this discrepancy reaches $\sim 15\%$.

Using the approximate second-order representation of the Molière distribution function (24)–(26) for computing the spectral radiation rate (79), the authors of [23] succeeded to agree satisfactorily theory and 25 GeV and 0.7% L_R data over the ω range 5 to 30 MeV.

This result can be understood by considering the fact that the correction of order of $1/B^B$ to the Gaussian first-order representation of the distribution function $w_M(\vartheta)$ is about 12% for the value used in calculations $B^B = 8.46$ [23].

Let us obtain the relative Coulomb correction to the average value of the spectral density of radiation for two limiting cases (82).

In the first case $\gamma^2\overline{\vartheta^2} \ll 1$, taking into account the equality

$$\delta_{\text{CC}}[\gamma^2\overline{\vartheta^2}] = \delta_{\text{CC}}[\overline{\vartheta^2}], \quad (83)$$

(65), and (82), we get

$$\delta_{\text{CC}} \left[\left\langle \frac{dI}{d\omega} \right\rangle \right] = \delta_{\text{CC}} \left[\left(\frac{dI}{d\omega} \right)_0 \right] = \frac{f(\xi)}{1 - B^B}, \quad (84)$$

where $B^B \approx 8.46$ in the conditions of the discussed experiment [23].

In the second case $\gamma^2\overline{\vartheta^2} \gg 1$, we have

$$\Delta_{\text{CC}} \left[\ln \left(\gamma^2\overline{\vartheta^2} \right) - 1 \right] = \Delta_{\text{CC}} \left[\ln \left(\overline{\vartheta^2} \right) \right] = \Delta_{\text{CC}} \left[\ln(B) \right]. \quad (85)$$

For the latter quantity, one can obtain

$$\Delta_{\text{CC}} \left[\ln(B) \right] = \Delta_{\text{CC}}[B] + f(Z\alpha) = \delta_{\text{CC}}[B]. \quad (86)$$

The Coulomb correction then becomes

$$\Delta_{\text{CC}} \left[\ln \left(\gamma^2\overline{\vartheta^2} \right) - 1 \right] = \frac{\delta_{\text{CC}}[B]}{\left[\ln \left(\gamma^2\overline{\vartheta^2} \right)^B - 1 \right]}. \quad (87)$$

Taking into account (65), we arrive at a result:

$$\delta_{\text{CC}} \left[\left\langle \frac{dI}{d\omega} \right\rangle \right] = \frac{f(\xi)}{\left[\ln \left(\gamma^2\overline{\vartheta^2} \right)^B - 1 \right] \left(1 - B^B \right)}. \quad (88)$$

The numerical values of these corrections are presented in Table 10.

The second asymptote is not reached [23] in the experiment [15, 16]. Therefore, we will now consider another limiting case corresponding to this experiment

Table 10. The relative Coulomb correction $\delta_{\text{CC}}[\langle dI/d\omega \rangle]$ to the asymptotes of the Born spectral radiation rate over the range $\omega < \omega_c$ for $\beta = 1$, $B^B \approx 8.46$, and $(\gamma^2\overline{\vartheta^2})^B \approx 7.61$ [23]

Target	Z	$\gamma^2\overline{\vartheta^2}$	$-\delta_{\text{CC}}[\langle dI/d\omega \rangle]$	R_{CC}
Au	79	$\gamma^2\overline{\vartheta^2} \ll 1$	0.042	0.958
Au	79	$\gamma^2\overline{\vartheta^2} \gg 1$	0.040	0.960

and taking into account the second term of the Molière distribution function expansion (19).

Substituting the second-order expression (24) for the distribution function in (79) and integrating its second term (25), we can arrive at the following expression for the electron radiation spectrum at $\mu^2 = \gamma^2 \vartheta^2 \gg 1$ [23]:

$$\left\langle \frac{dI}{d\omega} \right\rangle = \frac{2e^2}{\pi} \left\{ \ln(\mu^2) - C_E \left(1 + \frac{2}{\mu^2} \right) + \frac{2}{\mu^2} + \frac{C_E}{B} - 1 \right\}. \quad (89)$$

In order to obtain the Coulomb correction to the Born spectral radiation rate from (89), we first calculate its numerical value at $(\mu^2)^B \approx 7.61$ and $B^B \approx 8.46$, and we become $\langle dI/d\omega \rangle^B = 0.00542$. The Bethe–Heitler formula in the Born approximation gets $\langle dI/d\omega \rangle_{\text{BH}}^B = 0.00954$.

Then, we calculate the numerical values of B and μ^2 parameters including the Coulomb corrections. From

$$\Delta_{\text{CC}}[B] = \frac{f(\xi)}{1/B^B - 1} = -0.355, \quad (90)$$

we obtain $B = 8.105$ for $Z = 79$ and $B^B \approx 8.46$. The equality

$$\Delta_{\text{CC}}[\ln \mu^2] = \Delta_{\text{CC}}[\ln B] = \Delta_{\text{CC}}[B] + f(\xi) = \delta_{\text{CC}}[B] = -0.042 \quad (91)$$

gets $\ln \mu^2 = 1.987$ and $\mu^2 = 7.295$. Substituting these values in (89), we have $\langle dI/d\omega \rangle = 0.00531$. The relative Coulomb corrections to these parameters are presented in Table 11. These corrections are not large. Their sizes are between two and four percent, i.e., of order of the experimental error.

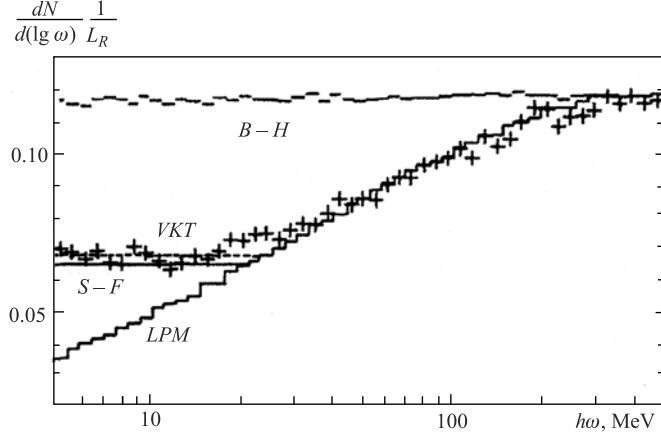
Table 11. The relative Coulomb corrections in the analogue of the LPM effect theory for $0.07 L_R$ gold target, $\omega < \omega_c$, and $\beta = 1$

$\delta_{\text{CC}}[B]$	$\delta_{\text{CC}}[\ln \mu^2]$	$\delta_{\text{CC}}[(dI/d\omega)_0]$	$\delta_{\text{CC}}[\langle dI/d\omega \rangle]$	$\delta_{\text{CC}}[\Phi(s)]$
-0.042	-0.021	-0.042	-0.020	-0.021

Accounting for the relative Coulomb correction to the Bethe–Heitler spectrum of bremsstrahlung, we find $(dI/d\omega)_{\text{BH}} = 0.00916$. So we get

$$\left\langle \frac{dI}{d\omega} \right\rangle = 0.580 \left(\frac{dI}{d\omega} \right)_{\text{BH}}. \quad (92)$$

This leads to the value of the spectral radiation rate in terms of $dN/[d(\log \omega)] \times 1/L_R$, where N is the number of events per photon energy bin per incident electron, $dN/[d(\log \omega)/L_R] = 0.118 \cdot 0.580 = 0.068$ which agrees very well with the experimental result over the frequency range $\omega < 30$ MeV for 25 GeV electron beam and $0.7\% L_R$ gold target. This result additionally improves the agreement between the theory and experiment (see figure).



Measurement of the LPM effect over the range $30 < \omega < 300$ MeV and its analogue in the range $5 < \omega < 30$ MeV for the $0.7\%L_R$ gold target and 25 GeV electron beam. The signs '+' denote the experimental data; the histograms $B-H$ and LPM give the Bethe-Heitler and the LPM Monte Carlo predictions [15]. The solid and dashed lines ($S-F$ and VKT) over the range $\omega < 30$ MeV are the results of calculations without [23] and with the obtained Coulomb corrections

4. SUMMARY AND CONCLUSIONS

- Within the theory of LPM effect for finite-size targets, we calculated the Coulomb corrections to the Born bremsstrahlung rate $\langle dI(\omega)/d\omega \rangle^B$ and estimated the ratio $\langle dI(\omega)/d\omega \rangle / \langle dI(\omega)/d\omega \rangle^B = R(\omega, L)$ for gold target based on results of the revised Molière small-angle multiple scattering theory for the Coulomb corrections to the screening angle.

- We demonstrated that the $R(\omega, L)$ value coincides with the normalization constant R value for $0.7-6\%L_R$ (25 GeV) data over the ω range 30 to 500 MeV from [8, 15]; however, the latter ignores the dependence of the ratio on ω and L .

- We have obtained the analytical and numerical results for the Coulomb corrections to the function $\nu(\eta) = 2\pi \int \sigma_0(\theta)[1 - J_0(\eta\theta)]\theta d\theta$ and complex potential $U(\eta) = -\omega\lambda^2/2 - i n_0\nu(\eta)$ and showed that $-\delta_{CC}[\nu(\eta)] = -\delta_{CC}[U(\eta)] \sim 4.3\% < -\delta_{CC}[\langle dI/d\omega \rangle] \sim 8.0\%$ for $Z = 79$ ($\beta = 1$).

- Additionally, we found Coulomb corrections to the quantities of the Migdal LPM theory and some important parameters of the Molière multiple scattering theory: $\Delta_{CC}[(dI/d\omega)_0]$, $\Delta_{CC}[q]$, $\Delta_{CC}[s^2]$, $\Delta_{CC}[s]$, $\Delta_{CC}[\Phi(s)]$, and $\Delta_{CC}[\langle dI/d\omega \rangle]$.

- We also calculated relative Coulomb corrections $\delta_{CC}[(dI/d\omega)_0] = \delta_{CC}[q] = \delta_{CC}[\overline{v^2}] = \delta_{CC}[B]$ and estimated $\delta_{CC}[\Phi(s)] = \delta_{CC}[s]$ as well as $\delta_{CC}[\langle dI/d\omega \rangle]$

for $s \ll 1$ and $Z = 79$ ($\beta = 1$). So we demonstrated that the latter correction $\delta_{CC} [\langle dI/d\omega \rangle]$ comprises the order of 14% at minimum B^B value 4.5.

- We demonstrated that the average value -5.4% of the relative Coulomb correction for $Z = 79$ coincides with the normalization correction value $(-5.5 \pm 0.2)\%$ for $6\%L_R$ gold target obtained in the experiment [16].

- We have performed analogous calculations for the regime of small LPM suppression over the entire range $1 \leq s \leq \infty$, and we found that the values of the Coulomb corrections $\delta_{CC} [\langle dI/d\omega \rangle] = (-4.50 \pm 0.05)\%$ ($Z = 82$) and $\delta_{CC} [\langle dI/d\omega \rangle] = (-5.35 \pm 0.06)\%$ ($Z = 92$) coincide with the values of the normalization correction $(-4.5 \pm 0.2)\%$ for $2\%L_R$ lead target and $(-5.6 \pm 0.3)\%$ for $3\%L_R$ uranium target, respectively, within the experimental error.

- The sample average over the range $1 \leq s \leq \infty$, $\bar{\delta}_{CC} [\langle dI/d\omega \rangle] = (-4.70 \pm 0.49)\%$, excellently agrees in the regime of small LPM suppression with the mean normalization correction $(-4.7 \pm 2)\%$ obtained for 25 GeV data in the experiment [16].

- Thus, we managed to show that the discussed discrepancy between theory and experiment can be explained both qualitatively and quantitatively on the basis of the obtained Coulomb corrections to the Born bremsstrahlung rate within the Migdal LPM effect theory.

- We found that applying the revised small-angle multiple scattering theory by Molière allows one to avoid multiplying theoretical results by above normalization factor and leads to agreement between the theory of LPM effect and experimental 25 GeV data for sufficiently thick targets over the range $30 < \omega < 500$ MeV with an accuracy about one percent.

- We evaluated the accuracy of the Fokker–Planck approach and the Gaussian first-order representation of the distribution function $w_0(\vartheta)$ in the limiting case $\omega = 0$ and showed the need of accounting for the second-order correction of order of $1/B^B \sim 12\%$ for $w(\vartheta)$ to eliminate the discrepancy between the theory and experiment over the frequency range $5 < \omega < 30$ MeV for 25 GeV and $0.7\%L_R$ data of the experiment [15, 16].

- Finally, we found the numerical values of the relative Coulomb corrections $\delta_{CC} [(dI/d\omega)_0]$, $\delta_{CC} [\Phi(s)]$, and $\delta_{CC} [\langle dI/d\omega \rangle]$ in the LPM effect theory analogue for a thin target and demonstrated that these corrections additionally improve the agreement between the theory [22, 23] and experiment [15, 16].

REFERENCES

1. Landau L. D., Pomeranchuk I. Ya. // Proc. Russ. Acad. Sci. 1953. V. 92. P. 535, P. 735 (in Russian) [Translated into English: In The Collected Papers of L. D. Landau, New York: Pergamon Press, 1965. P. 589].
2. Migdal A. B. // Proc. Russ. Acad. Sci. 1954. V. 96. P. 49.

3. Migdal A. B. // Phys. Rev. 1956. V. 103. P. 1811; JETP. 1957. V. 32. P. 633.
4. Goldman I. I. // JETP. 1960. V. 38. P. 1866.
5. Baier V. N., Katkov V. M., Strakhovenko V. M. // JETP. 1988. V. 67. P. 70.
6. Baier V. N., Katkov V. M. // Phys. Rev. D. 1998. V. 57. P. 3146.
7. Blencenbeckler R., Drell S. D. // Phys. Rev. D. 1996. V. 53. P. 6265; Blencenbeckler R. // Phys. Rev. D. V. 55. P. 190. 1997.
8. Zakharov B. G. // JETP Lett. 1996. V. 64. P. 781.
9. Shul'ga N. F., Fomin S. P. // JETP Lett. 1978. V. 27. P. 117;
Shul'ga N. F. // Int. J. Mod. Phys. A. 2010. V. 25. P. 9.
10. van Goethem M. J. et al. // Phys. Rev. Lett. 2002. V. 88. P. 122302.
11. Kopeliovich B. Z., Schäfer A., Tarasov A. V. // Phys. Rev. C. 1999. V. 59. P. 1609.
12. Gyulassy M., Wang X.-N. // Nucl. Phys. B. 1994. V. 420. P. 583;
Gyulassy M., Levai P., Vitev I. // Nucl. Phys. B. 2001. V. 594. P. 371.
13. Baier V. N., Katkov V. M. // Phys. Lett. A. 2006. V. 353. P. 91; arXiv:0711.3670, hep-ph.
14. Peigné S., Smilga A. V. // Advan. Phys. Sci. 2009. V. 179. P. 697.
15. Anthony P. L. et al. // Phys. Rev. Lett. 1995. V. 75. P. 1949; 1996. V. 76. P. 3550.
16. Anthony P. L. et al. // Phys. Rev. D. 1997. V. 56. P. 1373.
17. Hansen H. D. et al. // Phys. Rev. Lett. 2003. V. 91. P. 014801; Phys. Rev. D. 2004. V. 69. P. 032001.
18. Andersen J. U. et al. Electromagnetic Processes in Strong Crystalline Fields, CERN-SPSC-2005-030;
CERN-NA63 Collaboration // Phys. Lett. B. 2009. V. 672. P. 323; Nucl. Instrum. Meth. B. 2010. V. 268. P. 1412.
19. Tarasov A. V., Voskresenskaya O. O. // Alexander Vasilievich Tarasov: To the 70th Birth Anniversary. Dubna: JINR, 2012. P. 276–297; ArXiv:1107.5018 v 2, hep-ph;
Tarasov A. V., Voskresenskaya O. O. ArXiv:1204.3675, hep-ph.
20. Kuraev E. A., Voskresenskaya O. O., Tarasov A. V. JINR Preprint E2-2012-135. Dubna, 2012; ArXiv:1312.7809, hep-ph; Phys. Rev. D (submitted).
21. Molière G. // Z. Naturforsch. 1947. V. 2a. P. 133; 1948. V. 3a. P. 78; 1955. V. 10a. P. 177;
Bethe H. A. // Phys. Rev. 1953. V. 89. P. 256.
22. Shul'ga N. F., Fomin S. P. // JETP Lett. 1996. V. 63. P. 873.
23. Shul'ga N. F., Fomin S. P. // JETP Lett. 1998. V. 113. P. 58.
24. Feynman R. P., Hibbs A. R. Quantum mechanics and path integrals. New York: McGraw-Hill, 1965.
25. Voskresenskaya O. O. et al. JINR Preprint P2-97-308. Dubna, 1997 (in Russian);
Tarasov A. V., Torosyan H. T., Voskresenskaya O. O. ArXiv:1203.4853, hep-ph. 2012.
26. Scott W. T. // Rev. Mod. Phys. 1963. V. 35. P. 231.
27. Handbook of Mathematical Functions / Eds. M. Abramowitz and I. A. Stegun. National Bureau of Standards, Applied Mathematics Series, 1964.

Received on September 27, 2013.

Редактор *Е. И. Кравченко*

Подписано в печать 17.01.2014.

Формат 60 × 90/16. Бумага офсетная. Печать офсетная.

Усл. печ. л. 1,68. Уч.-изд. л. 2,2. Тираж 325 экз. Заказ № 58163.

Издательский отдел Объединенного института ядерных исследований
141980, г. Дубна, Московская обл., ул. Жолио-Кюри, 6.

E-mail: publish@jinr.ru

www.jinr.ru/publish/